Kelvin-Helmholtz Vortices and Double Mid-Latitude Reconnection at the Earth's Magnetopause: comparison between observations and simulations

Matteo Faganello, F. Califano, F. Pegoraro, Alessandro Retinò

Kelvin-Helmholtz Vortices and Double Mid-Latitude Reconnection at the Earth's Magnetopause: comparison between observations and simulations

M. Faganello[1], F. Califano[2], F. Pegoraro[2] and A. Retinò[3]

[1] *International Institute for Fusion Science/PIIM, UMR 7345 CNRS Aix-Marseille University, Marseille, France*
[2] *Phys. Dept., University of Pisa, Pisa, Italy*
[3] *LPP, CNRS/Ecole Polytechnique/UPMC/Paris-Sud 11, Palaiseau, France*

PACS 94.30.cp –
PACS 52.35.Mw –
PACS 52.65.Kj –

Abstract – Observational signatures of Kelvin-Helmholtz (K-H) vortices and of double mid-latitude reconnection are highlighted in satellite data of the THEMIS mission. It is shown that the plasma fluid quantities at the low-latitude flank of the Earth's magnetosphere are compatible with K-H vortices, as described by three-dimensional simulations. At the same time it is shown that the particle fluxes are compatible with the presence of magnetic field lines, embedded in the K-H vortices, that close on Earth but are connected to the solar wind at low-latitude. These field lines are generated during the K-H evolution by magnetic reconnection proceeding spontaneously in both hemispheres at mid-latitudes, allowing the solar wind plasma to enter the Earth's magnetosphere directly.

Accounting for the particle transport properties in dilute space or hot laboratory plasmas remains a difficult and open physics problem due to the low collisionality of such media that makes the plasma dynamics nonlocal. In particular, in quasi-collisionless magnetized systems such as the Earth's magnetosphere, the particle orbits are strongly related to the magnetic field lines. Or, from a fluid point of view, the large-scale magnetic field obeys a nearly ideal MagnetoHydroDynamic evolution maintaining its original connectivity to the different plasma regions. In such systems collisional cross field diffusion is usually negligible and anomalous diffusion related to wave activity can be too weak to explain the efficient mixing between "unconnected" plasma regions, that is observed in the case of the Earth's magnetosphere and the solar wind [1]. More specifically it is not straightforward to identify unequivocally the physical mechanisms underlining the efficient transport of solar wind plasma inside the magnetosphere when the magnetic field advected by the solar wind is mainly parallel to the Earth's dipole axis (northward periods) and the related formation of a cold and dense plasma sheet in the near-earth magnetotail [2, 3]. From a hydrodynamic point of view the anomalous diffusivity associated with Kelvin-Helmholtz vortices, growing along the flank of the magnetosphere during these periods [4], could explain the efficient transport properties of this boundary. However in an ideal MHD magnetized system, vortex development represents only a folding of the original boundary and a source for momentum transport [5], but cannot actually allow the solar wind plasma to penetrate the magnetosphere. For these reasons magnetic reconnection [6, 7] has been invoked as one of the few mechanisms able to explain the actual particle transport by changing the global magnetic field topology and thus creating flux tubes associated to magnetic field lines closed on Earth but partially populated by solar wind particles. At the same time Kinetic Alfvén Waves, which can be excited by surface waves, such as K-H vortices [8], or by compressional waves [9,10], can, if they have a sufficiently large amplitude, enhance the cross-field diffusion.

During northward periods magnetic reconnection can occur in the lobe regions [1, 11] and it has been proposed as a mechanism for the formation of the observed mixing layer [12, 13]. In particular the fact that particle fluxes parallel and anti-parallel to the local magnetic field were, or were not, balanced was used [13–17] as an indicator

of the field line topology, showing the transition from interplanetary "open" lines to lines connected to the Earth at only one pole and finally to lines "closed" by reconnection occurred in both lobes. In addition, in simplified 2D configurations that are not able to describe the actual topology of the magnetosphere-solar wind system, it has been shown that non-ideal effects such as anomalous resistivity or electron inertia can trigger magnetic reconnection during the evolution of K-H vortices [18–21]. However the former mechanism is strongly dependent on the north-south symmetry of the magnetospheric system and thus it may not always occur in the actual magnetospheric geometry. Concerning the latter mechanism, it has been shown that the evolution of K-H vortices and of the magnetic topology can be totally different in a 3D geometry where the system is stable against the K-H instability at high latitudes.

In order to overcome these problems and to explain the observed mixing, a new mechanism, namely the onset of double mid-latitude reconnection (DMLR), has been investigated in numerical simulations. DMLR [22] is related to the intrinsic 3D behaviour of the K-H instability at the flank of the magnetosphere, in particular to the differential advection of magnetic lines, driven by the development of K-H vortices in the equatorial region [22–26]. This process creates current sheets at mid-latitudes where reconnection naturally occurs almost simultaneously. In this way DMLR is able to close solar wind field lines on Earth and to populate the magnetosphere with cold and dense plasma. The main advantage of this mechanism is the fact that the occurrence of two different reconnection processes is a direct result of the dynamics of the magnetic field lines. Moreover its predicted efficiency appears to be able to account for the observed plasma transport [22,27]. Finally, signatures of K-H vortices at low latitude has recently been reported [28] and the observed particle fluxes are not compatible with magnetic reconnection acting locally but with reconnection occurring far away from the equatorial plane. Indeed the location of reconnection sites can be inferred looking at particle fluxes for different energies and angles with respect to the magnetic line direction [29].

In this letter we report clear signatures of K-H vortices at the low-latitude flank of the Earth's magnetosphere observed by the THEMIS C spacecraft crossing the boundary between the magnetosphere and the magnetosheath during a northward period. We show that the observed fluid plasma quantities are compatible with the characteristic profiles of K-H vortices, as predicted by 3D numerical simulations able to retain the expected high-latitude stabilization of K-H instability. Furthermore the particle fluxes are compatible with reconnection occurring at mid-latitude in both hemispheres and with the generation of double-reconnected field lines. We infer that these lines are created dynamically by DMLR acting during the nonlinear evolution of K-H vortices as described by 3D simulations and represent a direct path in for the solar wind into the magnetosphere. Finally, we discuss the competition between magnetic reconnection and KAWs for the generation of the observed fluxes and conclude that, for the considered period, reconnection must be considered as the most efficient mechanism.

The same THEMIS data were recently analyzed and similar conclusions on the K-H vortices were suggested [30]. On the contrary it was proposed a different scenario for the magnetic dynamics based on a "local" description of the equatorial region, that cannot account for the complex 3D dynamics we propose.

On 15 April 2008, the THEMIS C spacecraft [31], following its nearly equatorial orbit, was at the magnetosphere boundary for more than 2 hours, at $X_{GSM} \simeq -7$, $Y_{GSM} \simeq 18$ and $Z_{GSM} \lesssim 0$. In particular between 07:40 and 09:25 UT THEMIS C detected quasi-periodical oscillations of the plasma and of the electromagnetic fields at the magnetopause. During this period the interplanetary magnetic field was mostly northward, as reported by THEMIS B lying in the magnetosheath and by the ACE spacecraft lying in the solar wind (not shown). The observed quasi-periodical oscillations have a period that is roughly equal to 3-5min, as expected for K-H vortices at the magnetopause [4, 18, 20], and are characterized by alternating cold-dense and hot-tenuous structures, a bipolar velocity field and strong magnetic oscillations. Furthermore the variations of the total (magnetic + thermal) pressure are of the order of $0.15nPa$, as expected for rolled-up K-H vortices [32]. Note that these variations are larger than the difference between the "unperturbed" pressure values inside the Magnetosphere and the magnetosheath and thus are generated by the vortex compression/decompression and cannot be simple attributed to spatial displacements of the magnetospheric boundary.

In order to associate the observed oscillations to K-H vortices we compare the THEMIS C data to the numerical simulations of the flank magnetopause. In these numerical simulations we adopt a simplified 3D slab geometry, with the open inhomogeneity direction perpendicular to the magnetopause along the y axis, the northward direction along the z axis and the $-x$ direction aligned along the solar wind direction, as in the GSM coordinate system. We consider an ideal MHD equilibrium configuration that is able to model the high-latitude stabilization of the K-H instability. In this configuration all physical quantities are functions of the x-component of the vector potential, given by $A_{eq,x}(y,z) = [4/3\, y + L_z/\, 3\pi \sinh(2\pi y/L_z)\, \cos(2\pi z/L_z)]\,/2$ (all quantities are normalized to the ion skip depth d_i, the ion cyclotron frequency Ω_{ci} and the ion mass m_i) and are constant along x. In particular the equilibrium shear velocity and the density are given by $\mathbf{U}_{eq}(y,z) = U_0/2\,\{1 + \tanh[A_{eq,x}(y,z)/L_u]\}\,\hat{\mathbf{x}}$, $n_{eq}(y,z) = 1 - \Delta n/2\,\{1 - \tanh[A_{eq,x}(y,z)/L_u]\}$. Setting the box dimensions as $L_x = 24\pi$, $L_y = 60$ and $L_z = 120\pi$ and the half-width $L_u = 3$ we obtain a nearly northward magnetic field lying in the y, z plane and a velocity gradient stronger in the

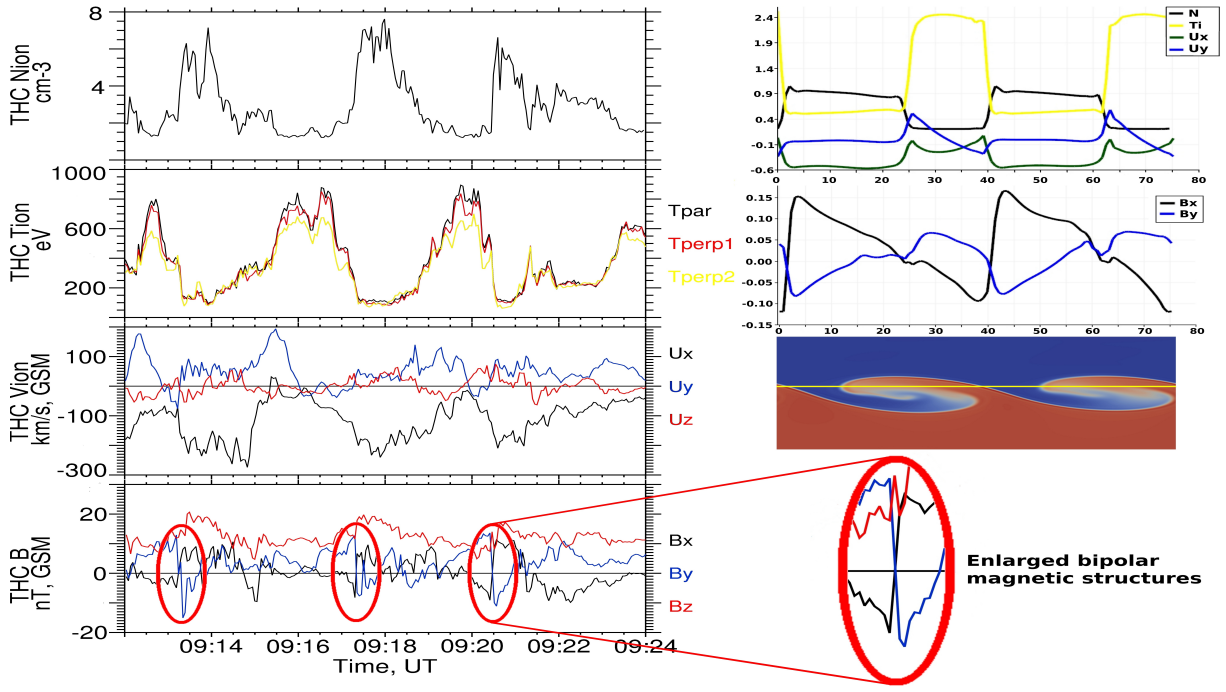

Fig. 1: Left column: ion density, temperature, bulk velocity and magnetic field as detected by THEMIS C. Right column: ion density, temperature and x, y components of the ion velocity and magnetic field obtained from a cut of the simulation box at $y = -5$, $z = -15$ and $t = 396$, corresponding to what would be seen by a stationary synthetic spacecraft surveying the tailward propagating vortices (yellow line in the third frame).

equatorial region than at high-latitudes. In this way the K-H instability grows much faster in the equatorial plane than at high latitudes [22,33] which can thus be considered as stable during the development of the instability at low latitude. In our simulations the Fast Growing Mode at the equator [34, 35] corresponds to $m_x = 2$ with m_x the wave number along the periodic x-direction. The reference values of the sound and Alfvén Mach numbers are set equal to $M_s = U_0/C_s = 1.3$, $M_A = U_0/U_A \simeq 1.0$, with $U_0 = 1.0$ and U_A the $+y$ asymptotic (magnetosheath) value of the equilibrium Alfvén velocity in the equatorial plane. The density jump between the two different regions ($y \gtrless 0$) is set equal to $\Delta n = 0.8$, reproducing the typical factor ~ 5 between the magnetosheath and the magnetospheric density and temperature (we assume a homogeneous thermal pressure for the equilibrium configuration). Note that the physical values considered here are not strictly equal to the observed values in the two different regions, indeed our 3D system represents only a modeling of the magnetospheric flank. Nevertheless the 3D model evolution is able to provide clear qualitative signatures of the K-H vortices that cannot be predicted by 2D models.

We describe the system evolution by adopting a Hall-MHD model that includes an adiabatic closure for the ion and electron temperatures, a small but finite resistivity ($\eta = 10^{-3}$ in normalized units) in the generalized Ohm's law [22] together with the diamagnetic term.

In Fig.1 we zoom in on three oscillations between 09:12 and 09:24 UT as a representative case. We show (left col-

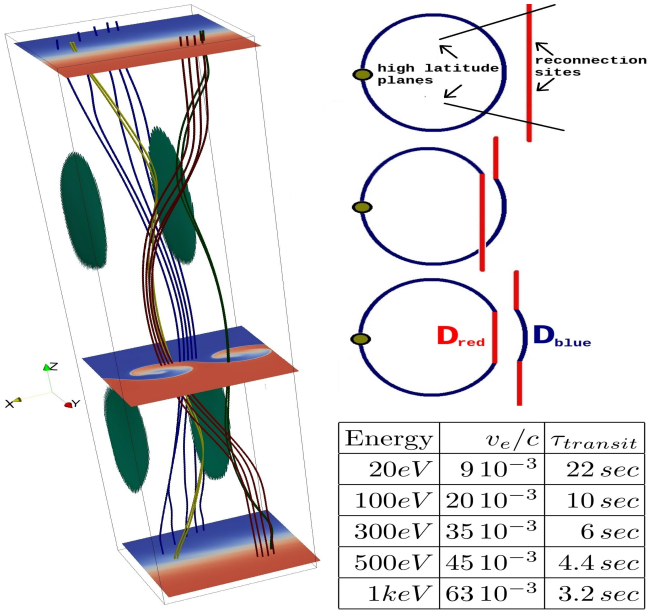

Energy	v_e/c	$\tau_{transit}$
$20eV$	$9\,10^{-3}$	$22\,sec$
$100eV$	$20\,10^{-3}$	$10\,sec$
$300eV$	$35\,10^{-3}$	$6\,sec$
$500eV$	$45\,10^{-3}$	$4.4\,sec$
$1keV$	$63\,10^{-3}$	$3.2\,sec$

Fig. 2: Left frame: ion density, represented in blue (tenuous) and red (dense), in the x, y-planes at $z = -180$, -15, $+180$, light green: current sheet isosurfaces defined by $|\mathbf{J}| = 0.8$, blue/red: pristine magnetospheric/magnetosheath field lines, green/yellow: "opened" and "newly closed" double reconnected field lines. Right frame: a schematic representation of DMLR and the values of $\tau_{transit}$ as a function of the electron energy.

umn) the observed values of the ion density, ion temperature, ion bulk velocity and of the magnetic field in GSM coordinates. The density and temperature exhibit the typical step-like structures associated with the cold-dense and hot-tenuous arms of the travelling vortices. The X_{GSM}-component of the ion velocity is tailward inside the high density arms and nearly zero inside the low density arms. The Y_{GSM}-component, roughly perpendicular to the magnetopause unperturbed surface, shows bipolar signatures inside the low density arms. These "fluid" profiles can be recognized in the numerical data (right column, upper frame) in a cut of the simulation box at $y = -5$, $z = -15$ and $t = 396$, corresponding to what would be seen by a synthetic spacecraft surveying the tailward propagating vortices. Furthermore the observed strong magnetic perturbations (left column, bottom frame) show a distinctive character, peculiar to the 3D evolution of K-H vortices. At each sharp transition between hot and cold regions (at 09:13:15, 09:17:20 and 09:21:00 UT) corresponding to the compressed transition region between different vortices close to the hyperbolic point of K-H instability, THEMIS C observes bipolar signatures of the X_{GSM}, Y_{GSM} components of the magnetic field. These special signatures are predicted by our 3D simulations (right column, second frame) and can be explained by the differential advection of initially northward directed magnetic field lines. In Fig.2, left frame, we show the plasma density together with the magnetic field lines at $t = 396$. The field lines are embedded into vortex structures grown in the low-latitude region and are advected at the vortex phase velocity, roughly one half the magnetosheath velocity. On the contrary, the feet of the blue magnetospheric and red magnetosheath field lines at high-latitudes are advected at the unperturbed velocity , i.e. in the magnetosheath they are advected by the flowing red plasma while in the stagnant blue magnetospheric plasma they are anchored. This differential advection bends and arches the magnetospheric and magnetosheath lines in opposite directions. From the point of view of a spacecraft surveying plasma and magnetic structures below the equatorial plane (plane at $z = -15$ in Fig.2), as in the case of THEMIS C, opposite arched blue and red field lines correspond to the detection of bipolar structures of the x, y magnetic components at the ribbons. The observed amplitudes of these structures are larger than the predicted ones. Nevertheless we must bear in mind that the dipolar structure of the global magnetospheric field and the draping of magnetosheath lines around the magnetopause [36], not included in our model, could enhance the arching effect at the near-tail flanks ($X_{GSM} \simeq -7$).

The differential line advection creates current sheets in both hemispheres at mid latitude (light green regions in Fig.2, left frame) where reconnection can develop. In fact reconnection occurs almost simultaneously in the northern and in the southern sheets and creates "newly closed" yellow lines that are connected to the blue magnetospheric plasma at high latitude, and thus to Earth, and to the red magnetosheath arm of K-H vortex at low-latitude. At the same time reconnection creates "opened" green lines, connected to the solar wind at high latitudes and to the magnetospheric plasma at low latitude.

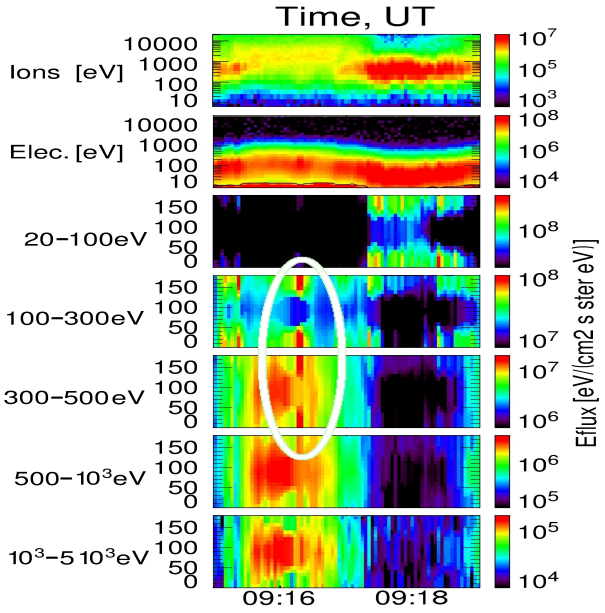

Fig. 3: First and second frames: ion and electron fluxes respectively, detected by THEMIS C, as a function of energy (eV) and time. Following frames: electron fluxes for different energy ranges, as a function of the pitch angle with respect to the local magnetic field. White ellipse shows the dense electron beams observed inside a magnetospheric arm at 09:16:20 UT.

We can find observational signatures of this magnetic dynamics by looking at the electron fluxes given as a function of the pitch angle with respect to the local magnetic field. For different energies, and corresponding parallel velocities, we compare the transit time $\tau_{transit}$ taken by electrons in order to escape/fill the segments D_{red} & D_{blue} (as defined in Fig.2, right frame) and the delay $\Delta t_{rec} \simeq 10sec$ between the two different reconnection processes along the same field line, as given by numerical simulations. We estimate the distance between the two reconnection sites as $\sim 1/6$ times ($\pm 30°$) the length of a circular line crossing the equator at the satellite position. Thus we obtain $L_{D_{red/blue}} \simeq 60000Km$ and the transit times, for different energies, given in Fig.2. This length is compatible with the distance between the stable planes in our simulations (at $z = \pm 180$) that we suppose to be $\sim 100000Km$ ($\pm 50°$).

In Fig.3, first and second frames, we show the ion and electron flux as a function of the particle energy. The cold-dense and the hot-tenuous regions map the different magnetospheric and magnetosheath arms of two close vortices accurately. In the following frames we show the electron fluxes in different energy ranges as a function of their pitch angle with respect to the local magnetic field. $20 - 100eV$ electrons are detected only inside the dense-cold region. On the contrary faster $100 - 500eV$ elec-

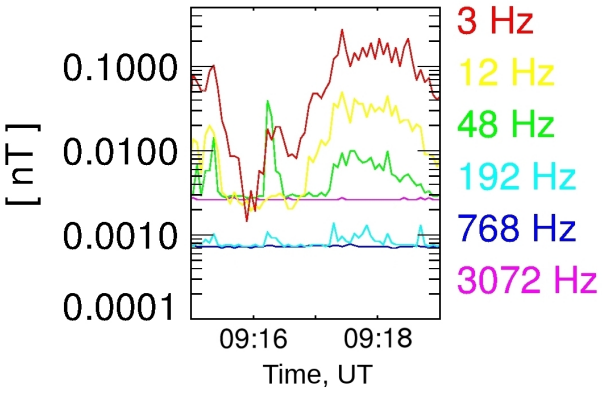

Fig. 4: Magnetic oscillation amplitudes for different frequencies, as reported by the Filter Bank.

trons, mainly coming from the magnetosphere, start to populate the cold region and show a dominant antiparallel component. Higher energy electrons are also present in the cold region but do not exhibit this anisotropy. These fluxes are compatible with DMLR that occurred first in the northern hemisphere some $15sec$ before their detection. In this case low energy electrons are too slow in order to escape from the magnetosheath segment D_{red} from where they originate or in order to populate the D_{blue} segment that crosses the hot-tenuous region. At intermediate energies electrons have enough time to fill the segment D_{red}, starting from the northern hemisphere where reconnection occurs first and therefore have unbalanced fluxes. Note that no strahl population is present in the magnetosheath during the considered period and thus cannot account for the observed fluxes. This anisotropy disappears at higher energies since these electrons are fast enough in order to populate D_{red} also from the southern hemisphere ($\tau_{transit}$ becomes smaller and smaller compared to $t_{detection} - t_{northern,rec} - \Delta t_{rec}$, i.e. $\tau_{transit} < t_{detection} - t_{southern,rec}$). Looking at the hot-tenuous region, we observe a partial depletion of parallel/antiparallel electrons with energy larger $\geq 300eV$. In fact these electrons have enough time to escape from the D_{blue} segment of "opened" tubes before their detection. Even more relevant is the observation of several parallel/antiparallel beams (the most visible is shown at 09:16:20 UT). The density in these beams is larger than the magnetospheric density in each energy range ($100eV$ up to $1000eV$). Thus we can suppose that these beams are composed of a magnetosheath dense population that is accelerated along field lines at the northern and southern reconnection sites. Indeed, once accelerated, these electrons have energies large enough to reach the satellite location in time to be detected.

In principle, bunch of accelerated electrons can also be produced along field lines by the parallel electric field of KAWs with long parallel wavelength. However, for the considered period, the KAW activity appears too weak to account for such an electron acceleration, as indicated by the observed magnetic wave amplitude at different frequencies (see Fig.ffig:waves). Indeed, the observed spectrum at 09:16:20 UT does not correspond to what would be obtained by KAW. For example, the dominant mode is detected at 48Hz, that would correspond to a doppler-shifted KAW with a too small wavelength, of the order of the electron skin depth. Instead, a KAW spectrum should be dominated by much larger wavelengths of the order of the ion Larmor radius [8–10]. Furthermore the observed wave activity at the beam location, or inside the magnetospheric arm (between 09:15:30 and 09:17:00 UT in Fig.4) or at the transition region between the magnetosphere and the magnetosheath, is too weak as compared to that typically reported when KAWs are recorded [8–10]. Finally, we do not observe on the data an enhancement of ion perpendicular temperature which would be a clear signature of KAWs. All these aspects lead us to conclude that, for the considered period, KAWs should be not responsible for the generation of the observed particle fluxes.

We also note that electron fluxes in the $20 - 100eV$ range differ from those usually observed inside the magnetosheath (that have a dominant perpendicular flux). Since the DMLR occurred too recently to affect these fluxes, we can suppose that the observed well-balanced parallel/antiparallel fluxes are related to the previous dynamics of the magnetopause (KAW activity or other phenomena). The same "lack of reaction" holds for ions: THEMIS C does not report any ion jet. This is expected in the case of recent reconnection at mid-latitude, since the accelerated ions are too slow to be observed at the satellite location. This fact is also confirmed by the lack of mixing between cold-dense and hot-tenuous ion populations inside the magnetospheric or magnetosheath arms, as shown in Fig.ffig:fluxes. Mixed ion populations are observed only at each transition region between the two different arms, where plasma density increases/decreases. These observations are consistent with the picture of vortices that grow on a pre-existing transition region (day-side magnetopause) and that, during their evolution, have folded the original boundary but, for the moment, not yet allowing an enhancement in the ion transport. The temporal width of these transition regions ($20-60sec$), that could be compressed near the hyperbolic point or decompressed inside each vortex during the K-H evolution, is compatible with the observed periods of K-H vortices ($3-5min$) [4].

It is worth noting that the generation of double-reconnected lines as a pairs of "opened" and "newly closed" lines is not only suggested by the simulations. This mechanism is strongly supported by physical arguments: once reconnection occurred in the northern hemisphere the resulting lines become braided at mid-latitude in the southern hemisphere. Reconnection must thus take place a second time between the same lines in order to unbraid them and reduce the line stretching [22].

In conclusion observational data are in agreement with a scenario where DMLR started to "close" interplanetary

field lines on Earth several seconds before the detection of the particle fluxes. We can thus expect that this new magnetic topology allows thermal solar wind ions and electrons to enter the magnetosphere since they can move along the "newly closed" field lines. In particular the redistribution of these low-energy and dense particle populations is expected to happen slightly tailward with respect to the satellite location and can account for the formation of a cold and dense plasma sheet in the near-earth magnetotail.

* * *

The research leading to these results received funding from the European Commission's Seventh Framework Programme (FP7/2007-2013) under the grant agreement SWIFF (project n. 263340, www.swiff.eu). This work was supported by the Italian Supercomputing Center - CINECA under the ISCRA initiative. We acknowledge NASA contract NAS5-02099 and V. Angelopoulos for use of data from the THEMIS Mission, O. LeContel and P. Henri for valuable suggestions for the treatment of electron fluxes. Part of data analysis was done with the AMDA science analysis system (http://amda.cdpp.eu/). We acknowledge the access to supermuc machine at LRZ made available within the PRACE initiative receiving funding from the European Commission's Seventh Framework Programme (FP7/2007-2013) under, Grant Agreement No. RI-283493, Project n. 2012071282.

REFERENCES

[1] G.C. Le *et al.*, J. Geophys. Res. **99**, 23723 (1994).
[2] T. Terasawa *et al.*, Geophys. Res. Lett. **24**, 935 (1997).
[3] M. Oieroset *et al.*, Geophys. Res. Lett. **32**, L12S07 (2005).
[4] H. Hasegawa *et al.*, Nature **430**, 755 (2004).
[5] A. Miura, J. Geophys. Res. **89**, 801 (1984).
[6] B. Coppi, Phys. Lett. **11**, 226 (1964).
[7] J.A. Wesson, Nuclear Fusion **30**, 2545 (1990).
[8] C.C. Chaston *et al.*, Phys. Res. Lett. **99**, 175004 (2007).
[9] J.R. Johnson *et al.*, Geophys. Res. Lett. **28**, 4421 (2001).
[10] J.R. Johnson *et al.*, Geophys. Res. Lett. **28**, 227 (2001).
[11] J.T. Gosling *et al.*, J. Geophys. Res. **96**, 14097 (1991).
[12] P. Song *et al.*, J. Geophys. Res. **97**, 1411 (1992).
[13] T.G. Onsager *et al.*, J. Geophys. Res. **106**, 25467 (2001).
[14] M. Fujimoto *et al.*, J. Geophys. Res. **103**, 4391 (1998).
[15] B. Lavraud *et al.*, J. Geophys. Res. **110**, A06209 (2005).
[16] M.B. Bavassano Cattaneo *et al.*, J. Geophys. Res. **111**, A09212 (2006).
[17] J.P. McFadden *et al.*, Geophys. Res. Lett. **35**, L17S09 (2008).
[18] A. Otto *et al.*, J. Geophys. Res. **105**, 21175 (2000).
[19] T.K.M. Nakamura *et al.*, Adv. Space. Res. **37**, 522 (2006).
[20] K. Nykyri *et al.*, Ann. Geophys **24**, 2619 (2006).
[21] M. Faganello, *et al.*, Phys. Rev. Lett. **101**, 175003 (2008).
[22] M. Faganello *et al.*, Europhys. Lett. **100**, 69001 (2012).
[23] J.U. Brackbill *et al.*, Phys. Rev. Lett.**86**, 2329 (2001).
[24] D. A. Knoll *et al.*, Phys. Plasmas **9**, 3775 (2002).
[25] C. Hashimoto *et al.*, Adv. Space. Res **37**, 527 (2006).
[26] K. Takagi *et al.*, J. Geophys. Res. **111** A08202 (1998).
[27] J. Labelle *et al.*, Space Sci. Rev. **47**, 175 (1988).
[28] M.B. Bavassano Cattaneo *et al.*, Ann. Geophys. **28**, 893 (2010).
[29] Y.V. Khotyaintsev, Yu. V. *et al.*, Phys. Rev. Lett. **97**, 205003 (2006).
[30] T.K.M. Nakamura *et al.*, J. Geophys. Res. **118**, 1 (2013).
[31] V. Angelopoulos *et al.*, Space Sci. Rev. **141**, 453 (2008).
[32] H. Hasegawa, Monogr. Environ. Earth Planets **1**, 71 (2012).
[33] M. Faganello *et al.*, Plasma Phys. Control. Fusion **54**, 124037 (2012).
[34] A. Miura, Phys. Rev. Lett. **16**, 779 (1982).
[35] A. Miura, Phys. Plasmas **4**, 2871 (1997).
[36] J. R. Spreiter *et al.*, Planet. Space Sci. **14**, 223 (1966).